

# AC Conductivity and Dielectric Properties of Borotellurite Glass

T.A. TAHA<sup>1,3</sup> and A.A. AZAB<sup>2</sup>

1.—Physics and Engineering Mathematics Department, Faculty of Electronic Engineering, Menoufia University, Menouf 32952, Egypt. 2.—Solid State Electronics Laboratory, Solid State Physics Department, Physics Division, National Research Centre, 33 El Bohouth St., Dokki, Giza P.O.12622, Egypt. 3.—e-mail: taha.hemida@yahoo.com

Borotellurite glasses with formula  $60\text{B}_2\text{O}_3-10\text{ZnO}-(30-x)\text{NaF}-x\text{TeO}_2$  ( $x = 0$  mol.%, 5 mol.%, 10 mol.%, and 15 mol.%) have been synthesized by thermal melting. X-ray diffraction (XRD) analysis confirmed that the glasses were amorphous. The glass density ( $\rho$ ) was determined by the Archimedes method at room temperature. The density ( $\rho$ ) and molar volume ( $V_m$ ) were found to increase with increasing  $\text{TeO}_2$  content. The direct-current (DC) conductivity was measured in the temperature range from 473 K to 623 K, in which the electrical activation energy of ionic conduction increased from 0.27 eV to 0.48 eV with increasing  $\text{TeO}_2$  content from 0 mol.% to 15 mol.%. The dielectric parameters and alternating-current (AC) conductivity ( $\sigma_{ac}$ ) were investigated in the frequency range from 1 kHz to 1 MHz and temperature range from 300 K to 633 K. The AC conductivity and dielectric constant decreased with increasing  $\text{TeO}_2$  content from 0 mol.% to 15 mol.%.

**Key words:** Borotellurite glasses, dielectric properties, electrical conductivity

## INTRODUCTION

Borate glasses have significant importance as specialized materials. Their transparency and high chemical resistance make them useful for various applications, e.g., in the construction industry, and optical and chemical technology. Nowadays, they have potential for use in advanced applications as vitreous electrolytes in strong-state batteries, in electrooptic switches and waveguides, as magneto-optic materials, in chemical sensors, and as laser materials.<sup>1–6</sup> Addition of tellurite to  $\text{B}_2\text{O}_3$  glasses changes their physical properties through generation of interesting structural units and decreases the hygroscopic nature.<sup>6–9</sup> The alternating-current (AC) electrical properties of glasses depend not only on the mobile ions which cause the direct-current (DC) conductivity but also on other, relatively immobile ions, or dipoles, etc., which could form part of the glassy network. These different mechanisms may, owing to temperature and other conditions, overlap and add to each other, or they may

exist in different parts of the frequency spectrum.<sup>9</sup> The aim of this research is to investigate the structural, electrical, and dielectric properties of the new borotellurite glass matrix  $60\text{B}_2\text{O}_3-10\text{ZnO}-(30-x)\text{NaF}-x\text{TeO}_2$ .

## EXPERIMENTAL PROCEDURES

The  $60\text{B}_2\text{O}_3-10\text{ZnO}-(30-x)\text{NaF}-x\text{TeO}_2$  ( $x = 0$  mol.%, 5 mol.%, 10 mol.%, and 15 mol.%) glass series were synthesized by a thermal melting technique. This borotellurite glass matrix containing NaF has high moisture resistance and mechanical strength compared with traditional, alkali oxyborate glasses.<sup>11</sup> The required amounts of Analar-grade  $\text{B}_2\text{O}_3$ , ZnO, NaF, and  $\text{TeO}_2$  were blended to homogenize the powder, then melted in a porcelain crucible inside a muffle furnace under ordinary atmosphere at temperature of around 1150°C for 30 min. The melt was poured into a cylindrical-shaped stainless-steel mold to obtain samples with thickness of 2 mm. X-ray diffraction (XRD) measurements were conducted using a Philips PW 1373 diffractometer. Glass density ( $\rho$ ) was obtained using the Archimedes method at room

(Received November 16, 2015; accepted June 10, 2016; published online June 30, 2016)

temperature using toluene with accuracy of  $\pm 0.01 \text{ g/cm}^3$ . The molar volume ( $V_m$ ) was evaluated from the expression

$$V_m = \frac{\sum n_j M_j}{\rho}, \quad (1)$$

where  $x_j$  is the molar ratio of component  $j$ ,  $M_j$  is its molecular mass, and  $\rho$  is the mass density.

The DC electrical conductivity ( $\sigma$ ) for the present glass samples was measured utilizing a two-probe holder loaded into an electrical furnace; for good contacts with the copper terminals, the glass samples were painted on both sides with silver. A steady voltage of 300 V was applied between the two electrodes, and the current was measured using a Keithley 616 electrometer. The dielectric parameters and AC conductivity ( $\sigma_{ac}$ ) were measured using a Hioki LCR meter model 3532, as a function of temperature from 300 K to 650 K at different frequencies between 100 kHz and 5 MHz. The temperature was measured using a digital temperature controller equipped with chromel–alumel thermocouple.

## RESULTS AND DISCUSSION

XRD spectra of the prepared glass samples are illustrated in Fig. 1; no crystalline peaks were observed, confirming their amorphous nature. The

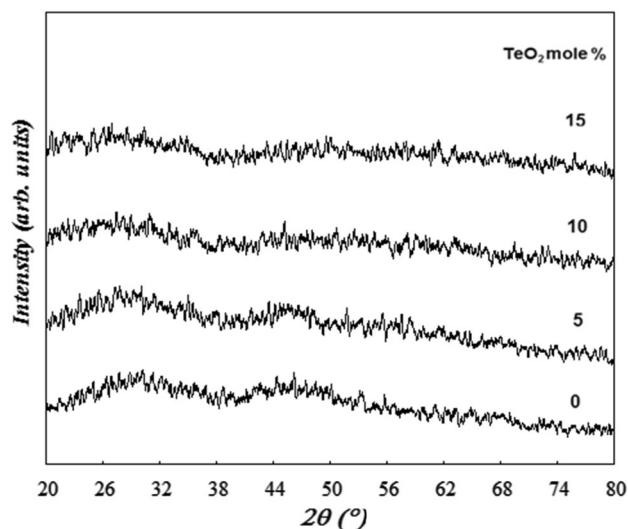


Fig. 1. XRD patterns for  $60\text{B}_2\text{O}_3-10\text{ZnO}-(30-x)\text{NaF}-x\text{TeO}_2$  glasses, where  $x$  is as indicated.

obtained values of glass density ( $\rho$ ) along with the molar volume  $V_m$  values are presented in Table I and illustrated in Fig. 2. The glass density increased linearly from  $2.52 \text{ g/cm}^3$  to  $2.74 \text{ g/cm}^3$  as the  $\text{TeO}_2$  content was increased from 0 mol.% to 15 mol.%. This increase in density with composition in the glass samples is because the molecular weight of  $\text{TeO}_2$  ( $159.60 \text{ g/mole}$ ) is larger than that of  $\text{NaF}$  ( $41.988 \text{ g/mol}$ ). The increase in molar volume might be due to increase in bond length or interatomic spacing between the atoms, and/or since the ionic radius of Te atom ( $2.21 \text{ \AA}$ ) is much greater than that of Na atom ( $0.97 \text{ \AA}$ ).<sup>10,11</sup> The average boron–boron separation  $d_{B-B}$  was evaluated to provide further insight into the present glassy network. As the boron atoms are the central atoms of  $\text{BO}_{3/2}$  and  $\text{BO}_{4/2}$  units, the volume  $V_m^B$  corresponding to one mole of boron atoms inside the glass structure is given by<sup>12,13</sup>

$$V_m^B = \frac{V_m}{2(1-y_B)}, \quad (2)$$

where  $y_B$  is the  $\text{B}_2\text{O}_3$  oxide mole fraction. The average boron–boron separation  $d_{B-B}$  was computed using the following formula and is recorded in Table I:

$$d_{B-B} = \left( \frac{V_m^B}{N_A} \right)^{\frac{1}{3}}, \quad (3)$$

where  $N_A$  is Avogadro's number,  $6.0228 \times 10^{23} \text{ g/mol}$ . The average boron–boron separation values  $d_{B-B}$  increased with increasing tellurium oxide content, so the glass system demonstrates an increasing tendency for expansion (less dense glass network).

The DC electrical conductivity in ionic conducting glasses at high temperatures<sup>14</sup> is observed to follow an Arrhenius relation,

$$\sigma = B \exp\left(-\frac{E_a}{k_B T}\right), \quad (4)$$

where  $B$  is a temperature-dependent preexponential factor,  $E_a$  is the mean electrical activation energy associated with the jump step during diffusion of ions in the studied temperature range,  $k_B$  is the Boltzmann constant, and  $T$  is absolute temperature. The activation energies for all the studied samples were evaluated from the slope of  $\log \sigma$  versus  $10^3/T$  curves (Fig. 3). The electrical activation energy,  $E_a$ , was found to increase from 0.27 eV to 0.48 eV with

Table I. Glass composition, density ( $\rho$ ), molar volume ( $V_m$ ), and average boron–boron separation ( $d_{B-B}$ )

Sample	Glass composition (mol.%)	$\rho$ ( $\text{g/cm}^3$ )	$V_m$ ( $\text{cm}^3/\text{mol}$ )	$d_{B-B}$ (nm)
T0	$60\text{B}_2\text{O}_3-10\text{ZnO}-30\text{NaF}$	2.5162	24.84	0.372
T5	$60\text{B}_2\text{O}_3-10\text{ZnO}-25\text{NaF}-5\text{TeO}_2$	2.6127	26.17	0.379
T10	$60\text{B}_2\text{O}_3-10\text{ZnO}-20\text{NaF}-10\text{TeO}_2$	2.6809	27.7	0.385
T15	$60\text{B}_2\text{O}_3-10\text{ZnO}-15\text{NaF}-15\text{TeO}_2$	2.7366	29.29	0.393

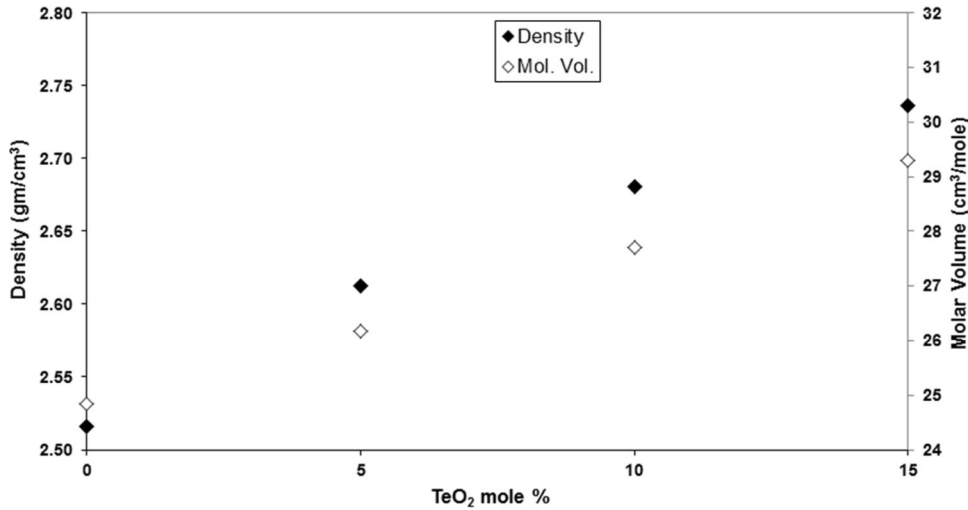


Fig. 2. Compositional dependence of density and molar volume.

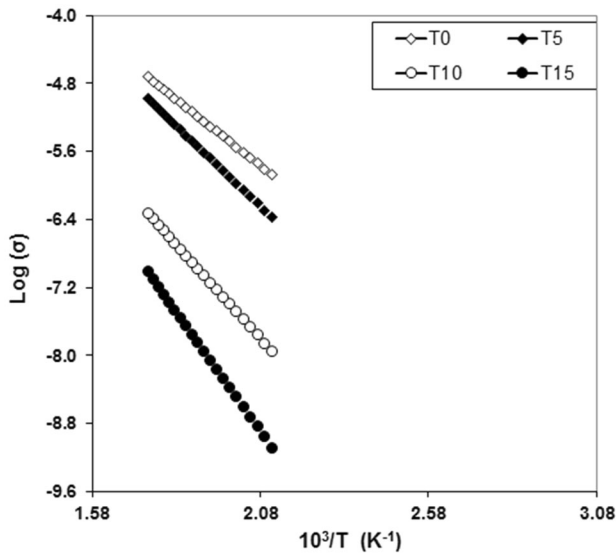


Fig. 3. Variation of  $\log \sigma$  against  $10^3/T$  for  $60\text{B}_2\text{O}_3-10\text{ZnO}-(30-x)\text{NaF}-x\text{TeO}_2$  glass.

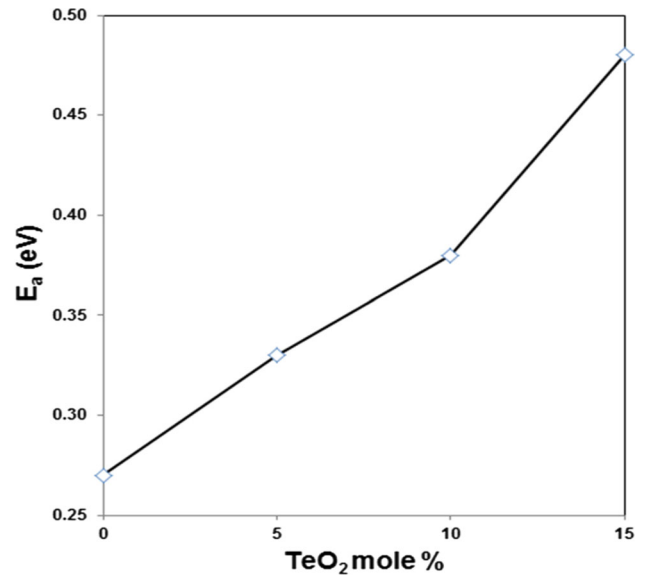


Fig. 4. Dependence of electrical activation energy on glass composition.

increasing TeO<sub>2</sub> mol.%, as shown in Fig. 4, which may be due to the decrease in Na<sup>+</sup> ion concentration.

Figure 5 shows frequency-dependent AC conductivity graphs ( $\ln \sigma_{ac}$  versus  $\ln f$ ) at various temperatures for the glass samples with  $x = 0$  mol.% and 15 mol.% TeO<sub>2</sub> as typical curves. The AC conductivity of the present glasses is observed to increase with frequency, which may be due to the increase of Na<sup>+</sup> mobile ion density.<sup>15</sup> The inset shows the variation of the AC conductivity with temperature at various frequencies. It is obvious that the AC conductivity is temperature dependent at low frequency but seems to be independent at high frequency. The frequency dependence of the AC

conductivity complies with Jonscher's universal power law<sup>15</sup>:

$$\sigma(\omega) = \sigma_{dc} + A\omega^s, \quad 0 < s < 1, \quad (5)$$

where  $\sigma_{dc}$  is the frequency-independent DC conductivity of the glass sample,  $A$  is a temperature-dependent parameter,  $\omega = 2\pi f$  is the angular frequency of the applied field, and  $s$  is the power-law exponent, which indicates the degree of interaction between mobile ions. The frequency dependence of the conductivity is the sum of the conductivity owing to diffusion of free charges (DC conductivity) and the polarization conductivity (AC conductivity) due to the motion of bound charges. The AC conductivity curves show a tendency to merge into

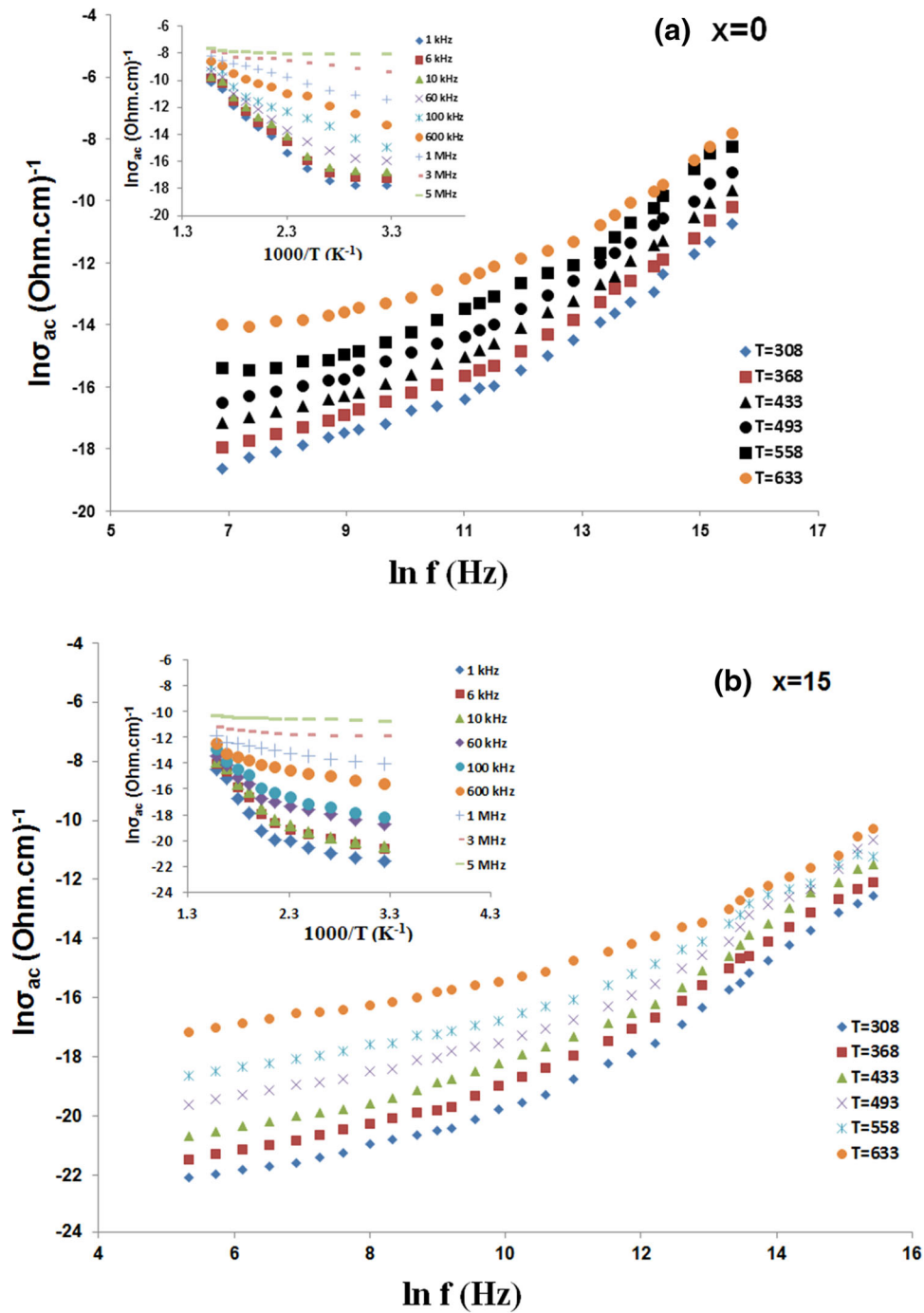


Fig. 5. Variation of  $\ln \sigma_{ac}$  versus  $\ln f$  at various temperatures for glass samples doped with (a) 0 mol.% and (b) 15 mol.%  $\text{TeO}_2$ .

**Table II. Glass composition and  $s$  value at different temperatures**

$s$						
$\text{TeO}_2$ mol.%	$T = 308$ K	$T = 368$ K	$T = 433$ K	$T = 493$ K	$T = 558$ K	$T = 633$ K
0	0.88	0.89	0.88	0.87	0.86	0.71
5	0.94	0.85	0.75	0.65	0.44	0.36
10	0.95	0.90	0.82	0.79	0.74	0.68
15	0.98	0.97	0.95	0.89	0.78	0.66

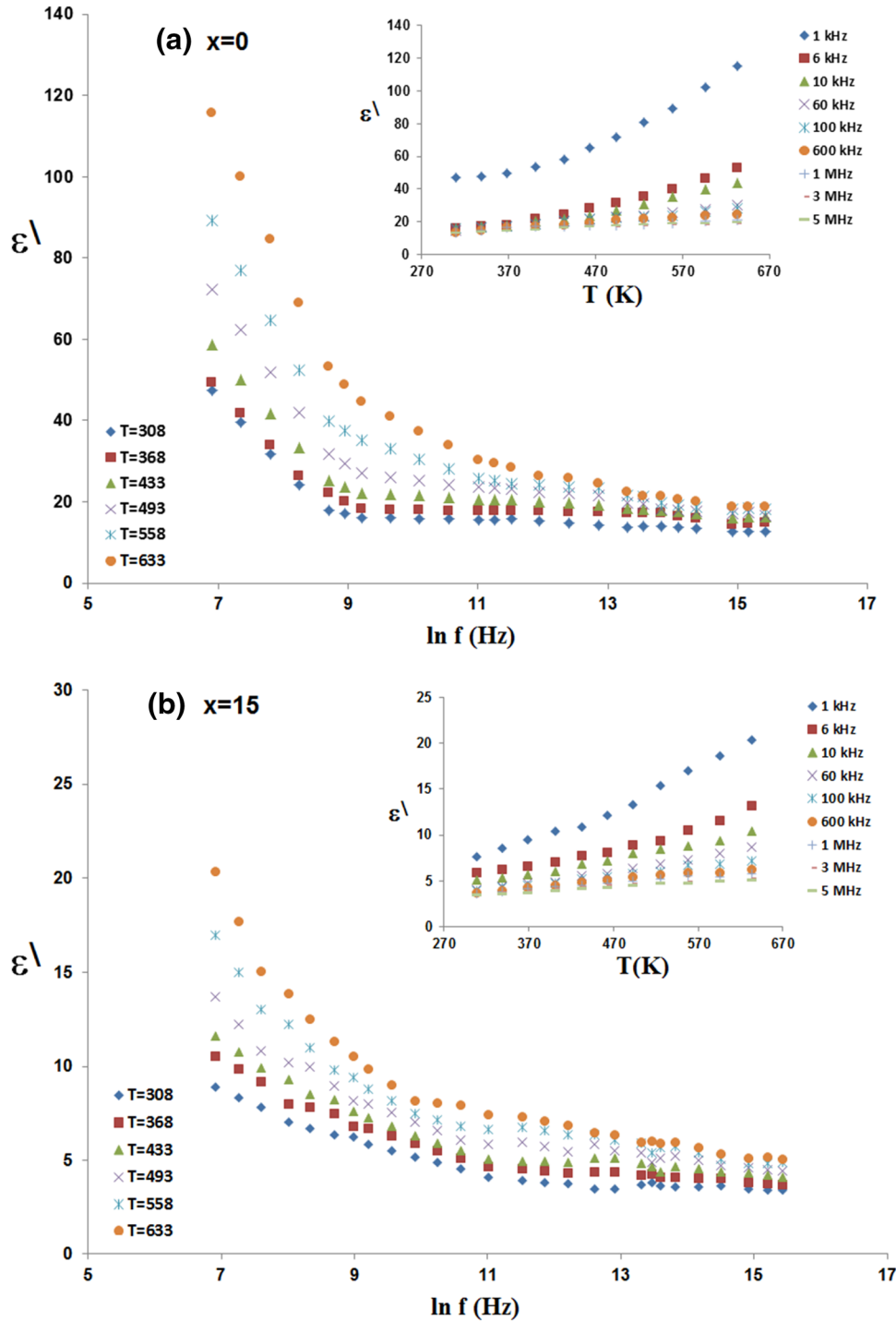


Fig. 6. Dielectric constant  $\epsilon'$  as a function of frequency at different temperatures for glass samples doped with (a) 0 mol.% and (b) 15 mol.%  $\text{TeO}_2$  content.

one curve at high frequency, as shown in Fig. 5; these curves show almost linear behavior, obeying the power-law equation<sup>16</sup>

$$\sigma(\omega) = A\omega^s. \quad (6)$$

Diverse models have been proposed to interpret the AC electrical conduction mechanism in glasses,

including:<sup>15,18</sup> (1) classical charge-carrier hopping over a barrier, for which the exponent  $s$  is constant with unity value; (2) the quantum-mechanical tunneling model, for which the exponent  $s$  takes the value 0.8 and is independent of or increases slightly with temperature; (3) the overlapping large-polaron tunneling model, for which the value of  $s$  depends on both frequency and temperature, decreasing to a

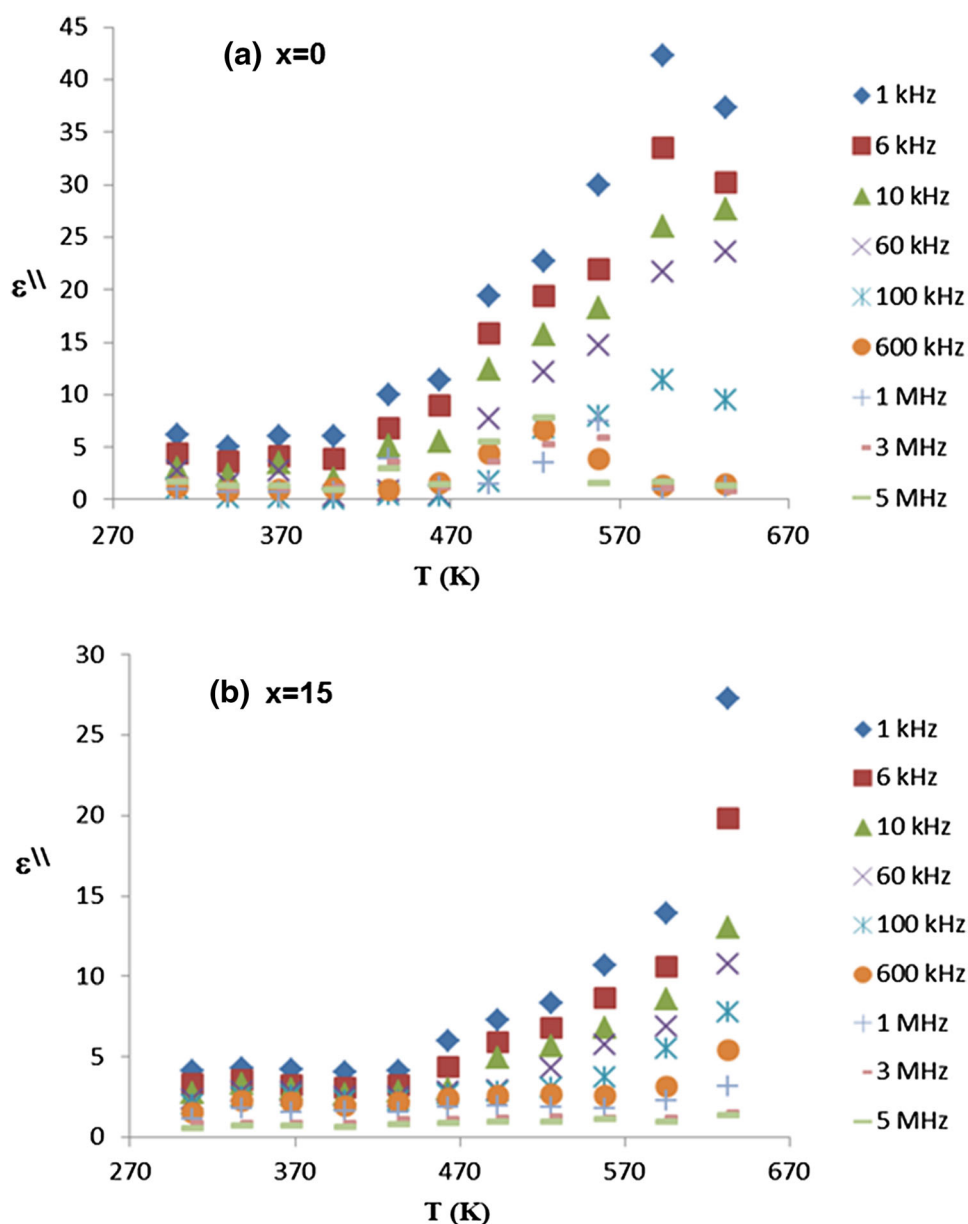


Fig. 7. Dielectric loss versus temperature for glass samples doped with (a) 0 mol.% and (b) 15 mol.% TeO<sub>2</sub>.

minimum value with rising temperature and increasing with further increase of temperature; (4) the correlated barrier hopping (CBH) model, for which the frequency exponent increases towards unity as the temperature decreases towards 0 K. The  $s$  values were calculated and are reported in Table II. The frequency exponent  $s$  is nearly temperature independent at around 0.8 for the sample with  $x = 0$ , suggesting that the quantum-mechanical tunneling model is applicable for  $x = 0$ . For the glass samples with  $x > 0$ , the exponent  $s$  decreases with temperature rise; such behavior can be seen in many amorphous semiconductors.<sup>15</sup> This behavior of  $s(T)$  indicates that correlated barrier hopping (CBH) is the rate-limiting electrical conduction

mechanism.<sup>14</sup> Also, one can note that the gradient of the  $s$  value for the sample with  $x = 5$  is higher than for the other samples. Since the frequency exponent  $s$  is assigned to the interaction between charge-carrier ions in the lattice, rapid decrease of  $s$  with temperature may be due to decreasing charge-carrier interaction in the lattice for this sample.

It is well understood that the dielectric properties of ionically conducting glass are due to electronic, ionic, and space-charge polarizations plus the dipole orientation contribution.<sup>17,18</sup> Charge carriers cannot move freely through glass, but they can be displaced (polarized) depending on the applied alternating electric field. The complex permittivity of glass is calculated using



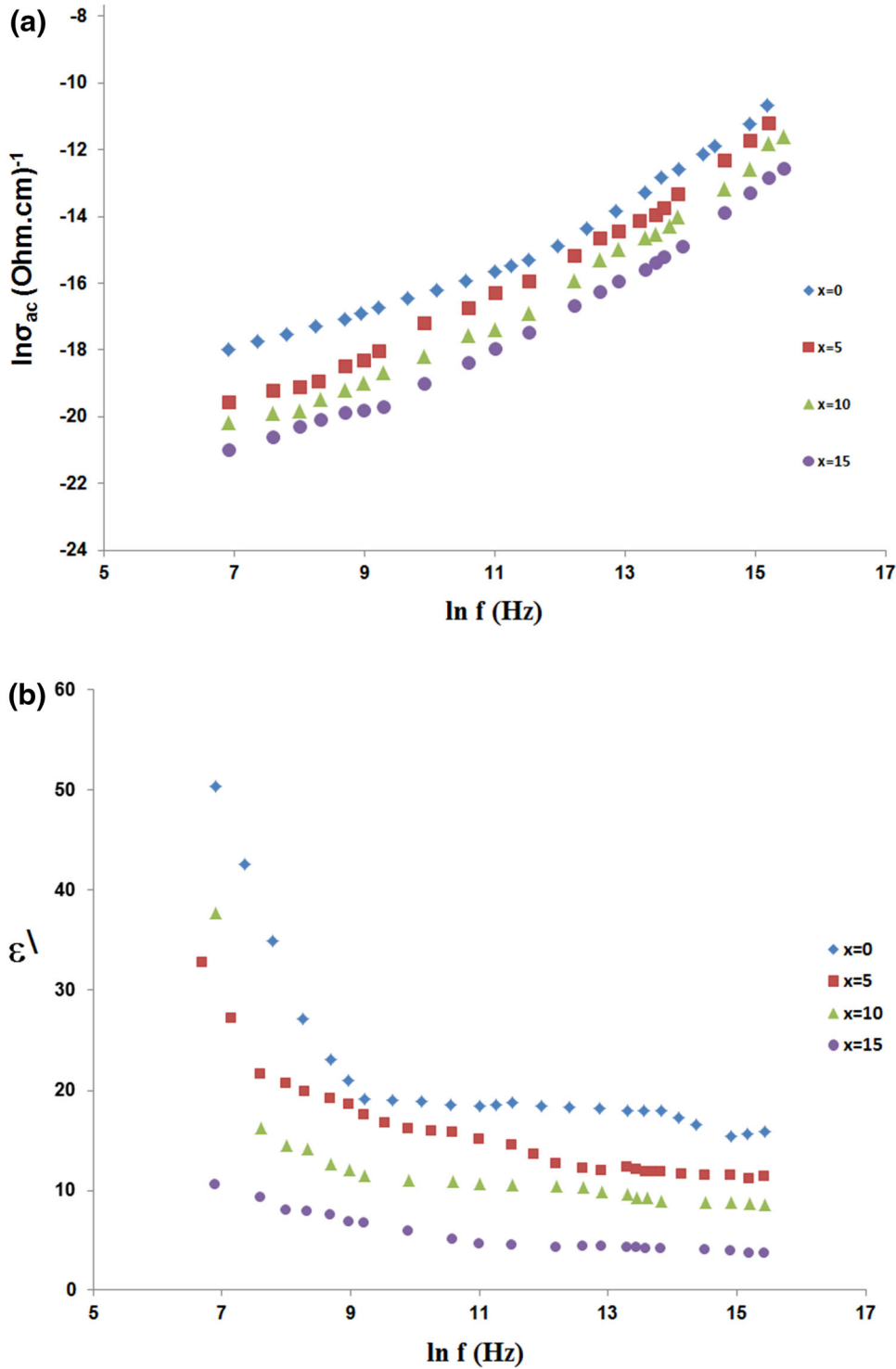


Fig. 8. Variation of (a) AC conductivity and (b) dielectric constant  $\epsilon'$  with frequency for different TeO<sub>2</sub> mole contents.

$$\epsilon^* = \frac{1}{(j\omega C_0 Z^*)} = \epsilon' - j\epsilon'' \quad (7)$$

where  $Z^*$  is the complex impedance and  $C_0$  is the free-medium capacitance. The real part of the permittivity (dielectric constant)  $\epsilon'$  is proportional to the polarizability (energy stored in the

material), while the imaginary part (dielectric loss)  $\epsilon''$  corresponds to the energy loss due to ionic conduction and polarization. The dielectric constant ( $\epsilon'$ ) is computed using

$$\epsilon' = \frac{Cd}{\epsilon_0 A} \quad (8)$$

where  $C$  is the measured capacitance,  $\epsilon_0$  is the free-space permittivity, and  $A$  is the surface area of the electrode, whereas the dielectric loss tangent is evaluated from the expression

$$\epsilon'' = \tan \delta \epsilon'. \quad (9)$$

Figure 6 demonstrates the variation of the dielectric constant  $\epsilon'$  with frequency at various temperatures for glass samples with  $x = 0$  mol.% and 15 mol.%  $\text{TeO}_2$  content as typical curves. It is noted that the dielectric constant  $\epsilon'$  decreased with increasing frequency. This behavior at low frequency may be attributed to polarizability arising from the contribution of the multiple components in the semiconductor glass materials. As the frequency increased, the ionic and orientation sources of polarizability decreased and finally disappeared because of the inertia of ions and molecules. The inset curves in Fig. 6 illustrate the increase in  $\epsilon'$  with temperature; at low temperatures, this behavior can be ascribed to small contributions of the electronic and ionic components, while the orientational component can be neglected. The electronic and ionic polarizability sources increased with increasing temperature as a result of the orientation and space-charge polarization contributions. Figure 7 shows that the dielectric loss decreased with increasing frequency and increased with temperature. At low frequency, this might be ascribed to migration of  $\text{Na}^+$  ions in the glass as the main reason for dielectric loss. Accordingly, the dielectric loss is characterized by high values at low and moderate frequencies because of the contribution of both wings (ion jump and conduction loss) of ion migration loss, in addition to electron polarization loss. At high frequencies, ion vibrations might be the main origin of dielectric loss.<sup>19</sup> The observed peaks of dielectric loss for the sample with  $x = 0$  can be predicted to occur when the charge hopping frequency is approximately equal to the external applied field frequency, in this case  $\omega\tau = 1$ , where  $\tau$  is the hopping process relaxation time and  $\omega$  is the angular frequency of the externally applied field ( $\omega = 2\pi f_{\text{max}}$ ).

Figure 8a shows the dependence of the AC conductivity on the  $\text{TeO}_2$  content in the composition. The AC conductivity decreased with increasing  $\text{TeO}_2$  content; this behavior can be explained in terms of the interstitial position of  $\text{TeO}_2$  inside the host matrix of the structure, which could impede ion motion. This behavior is supported by the increase of the activation energy with the  $\text{TeO}_2$  content, as shown in Fig. 3. Figure 8b demonstrates the decrease of the dielectric constant  $\epsilon'$  with increasing  $\text{TeO}_2$  content. This might be because the  $\text{TeO}_2$  decreases the space-charge polarization as well as the conductivity.

## CONCLUSIONS

Borate glasses with formula  $60\text{B}_2\text{O}_3 - 10\text{ZnO} - (30 - x)\text{NaF} - x\text{TeO}_2$  ( $x = 0$  mol.%, 5 mol.%, 10 mol.%, and 15 mol.%) were successfully prepared, and the amorphous nature of the samples was confirmed by XRD analysis. The DC conductivity of the samples decreased and the activation energy for ionic conduction increased from 0.27 eV to 0.48 eV with increasing  $\text{TeO}_2$  content from 0 mol.% to 15 mol.%, possibly due to decrease in  $\text{Na}^+$  ions. The AC conductivity and dielectric constant were found to decrease with increasing  $\text{TeO}_2$  content, making these glasses suitable for use in plasma display applications. The temperature dependence of the exponent  $s$  showed a decrease from 0.98 to 0.36 with increasing temperature from 308 K to 633 K; this behavior of  $s(T)$  suggests that correlated barrier hopping (CBH) is the rate-limiting conduction mechanism.

## REFERENCES

1. W. Beier and G.H. Frischat, *J. Non-Cryst. Solids* 73, 113 (1985).
2. K. Funke, *Prog. Solid State Chem.* 22, 111 (1993).
3. U. Schoo and H. Mehrer, *Solid State Ionics* 130, 243 (2000).
4. J.L. Piguet and J.E. Shelby, *J. Am. Ceram. Soc.* 68, 450 (1985).
5. I.W. Donald, B.L. Metcalfe, D.J. Bradley, M.J.C. Hill, J.L. McGrath, and A.D. Bye, *J. Mater. Sci.* 29, 6379 (1994).
6. Y.L. Yue, X.J. Yu, H.T. Wu, and X.J. Chen, *Mater. Res. Innovations* 13, 129 (2009).
7. S.P.H.S. Hashim, H.A. Sidek, M.K. Halimah, K.A. Matori, W.M.D.W. Yusof, and M.H.M. Zaid, *Int. J. Mol. Sci.* 14, 1022 (2013).
8. M.A. Khaled, H. Elzahed, S.A. Fayek, and M.M. El-Ocker, *Mater. Chem. Phys.* 37, 329 (1994).
9. R. El-Mallawany, *Tellurite Glasses Handbook, Physical Properties and Data* (Boca Raton: CRC Press, 2002), p. 540.
10. Y.B. Saddeek and L. Abd El Latif, *Phys. B* 348, 475 (2004).
11. A. Paul, *Chemistry of Glasses* (New York: Chapman and Hall, 1982), p. 102.
12. M.K. Murthy, K.S.N. Murthy, and N. Veeraiyah, *Bull. Mater. Sci.* 23, 285 (2000).
13. Y.B. Saddeek, *Mater. Chem. Phys.* 83, 222 (2004).
14. M.K. Halimah, H.A.A. Sidek, W.M. Daud, H. Zainul, Z.A. Talib, A.W. Zaidan, A.S. Zainal, and H. Mansor, *Am. J. Appl. Sci.* 2, 1541 (2005).
15. F. Berkemeier, S. Voss, A.W. Imre, and H. Mehrer, *J. Non-Cryst. Solids* 351, 3816 (2005).
16. M. Abdel-Baki, F.A. Abdel-Wahab, A. Radi, and F. El-Diasty, *J. Phys. Chem. Solids* 68, 1457 (2007).
17. N.F. Mott and E.A. Davis, *Electronic Processes in Non-crystalline Materials* (Oxford: Clarendon, 1979), p. 220.
18. V. Naresh and S. Buddhudu, *Ceram. Int.* 38, 2325 (2012).
19. A.K. Jonscher, *Nature* 267, 673 (1977).
20. S.R. Elliott, *Philos. Mag.* 36, 1291 (1977).
21. S.R. Elliott, *Adv. Phys.* 36, 135 (1987).
22. P. Nageswara Rao, B.V. Raghavaiah, D. Krishna Rao, and N. Veeraiyah, *Mater. Chem. Phys.* 91, 381 (2005).
23. R.V. Barde, K.R. Nemade, and S.A. Waghuley, *J. Asian Ceram. Soc.* 3, 116 (2015).
24. M.M. Elkholy and L.M. Sharaf El-Deen, *Mater. Chem. Phys.* 65, 192 (2000).